Journal of Power Sources 561 (2023) 232708

Contents lists available at ScienceDirect

Journal of Power Sources

journal homepage: www.elsevier.com/locate/jpowsour

Impact of feedstock dilution on the performance of urine-fed ceramic and membrane-less microbial fuel cell cascades designs

Xavier Alexis Walter [a,*], Jiseon You [b], Iwona Gajda [b], John Greenman [b], Ioannis Ieropoulos [c]

[a] Environmental and Biochemical Science Department, James Hutton Institute, Craigiebuckler, Aberdeen, AB15 8QH, UK
[b] Bristol Robotics Laboratory, University of the West of England, Coldharbour Lane, Bristol, BS16 1QY, UK
[c] Environmental Engineering Department, University of Southampton, University Road, Southampton, SO17 1BJ, UK

HIGHLIGHTS

- The ammonium removal rate positively correlated to the feedstock concentration.
- The organic removal rate negatively correlated to the feedstock concentration.
- Ceramic based designs have higher conversion efficiency than membrane-less designs.
- Membrane-less designs have higher performance than ceramic based designs.
- The presence of membranes limits the impact of urine dilution.

GRAPHICAL ABSTRACT

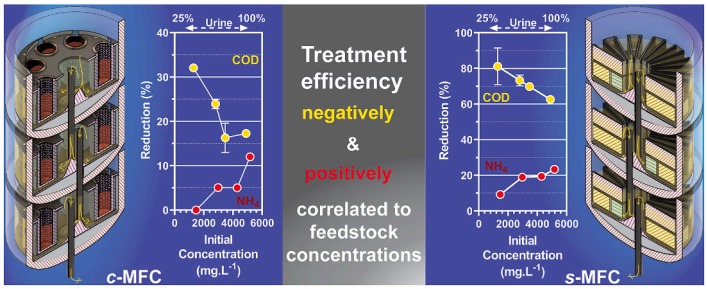

ABSTRACT

Recent advancements in the microbial fuel cell (MFC) field have led to the deployment of pilot-scale autonomous sanitation systems converting the organic content of urine into electricity to power lights in decentralised areas. Two designs have been deployed successfully, namely ceramic cylinder based MFCs ***(c-MFC)*** and membrane-less self-stratifying MFCs ***(s-MFC)***, but only one research has tested simultaneously these two designs under similar conditions. To complement this single study, the present work investigated the response of these two designs to the dilution of feedstock. Both designs were assembled as cascades, a configuration close to the conditions of implementation. The tested conditions were 100%, 75%, 50%, 25% urine diluted with tap water. Results have shown that under the 100% condition (neat urine), the ***s-MFC had a higher energy output*** *(2.29 ± 0.04 kJ* d^{-1}*)* ***and treatment*** *(4.16 ± 0.15* $g_{COD}.d^{-1}$*; 1.39 ± 0.15* $g_{NH4}.d^{-1}$*)* ***than the c-MFC.*** Under the 25% condition, the ***c-MFC had a higher energy output*** *(0.75 ± 0.04 kJ* d^{-1}*)* ***but a lower treatment*** *(0.40 ± 0.05* $g_{COD}.d^{-1}$*; 0.01 ± 0.02* $g_{NH4}.d^{-1}$*)* ***than the s-MFC.*** Both type of cascade designs could be fed a 75% concentration feedstock for a week without a significant performance decrease. Overall, the ***c-MFC cascade had higher*** energy conversion efficiency ***and the s-MFC had higher power generating performance.***

1. Introduction

With the growing pressure of time to limit the world temperature increase to a maximum of 1.5 °C above the pre-industrial baseline (c.a. average over the years 1850–1900) by 2050, every sector is under high pressure to decease its carbon footprint. Because of the interfaces of water and sanitation domains, the wastewater treatment sector, which is key to our modern societies, is also under pressure to reduce its carbon balance. Moreover, safe sanitation for everyone is also a major challenge worldwide. The microbial fuel cell (MFC) technology, as one of the

* Corresponding author.
E-mail addresses: alexis.walter@hutton.ac.uk (X.A. Walter), Jiseon.You@uwe.ac.uk (J. You), iwona.gajda@uwe.ac.uk (I. Gajda), john.greenman@uwe.ac.uk (J. Greenman), I.Ieropoulos@soton.ac.uk (I. Ieropoulos).

https://doi.org/10.1016/j.jpowsour.2023.232708
Received 21 October 2022; Received in revised form 21 December 2022; Accepted 14 January 2023
Available online 26 January 2023

potential solutions to these challenges, has received much attention. Although discovered in 1911 by M C. Potter [1], the technology has gained increasing interest since the years 2000 [2,3]. This interest has risen because the MFC technology can treat waste in an energy-neutral manner with the potential to be energy-positive depending on the implementation context.

The MFC technology relies on the anaerobic respiration of microorganisms able to employ an inert and conductive material as the end terminal electron acceptor of their heterotrophic respiration. When such material is connected to another spatially separated and conductive material that is able to transfer these electrons to an oxidised chemical element, an electrical current is generated. MFC reactors are energy transducers able to convert the energy contained in reduced organic matter into electrical energy. An MFC reactor comprises an anode, a cathode and typically a cation exchange membrane. In such reactors, the anaerobic electroactive microorganisms use the anode electrode as their electron acceptor when mineralising organic matter. The electrons pass through an external circuit, arrives at the cathode, and react with a compound of a higher redox potential (e.g. oxygen, ferricyanide) and cations (e.g. H_3O^+, NH_3^+, Na^+, K^+)), thus producing a current. Over the last two decades, many MFC reactor designs have emerged, depending on the targeted end-applications [4–10].

Urine brings 10% of the COD (i.e chemical oxygen demand, an indirect measure of the dissolved organic carbon), 75–80% of nitrogen; 45–50% of the phosphorous and 70% of the potassium found in municipal wastewater [11–13], whilst having a high electroconductivity comprised between 25 and 32 mS cm^{-2}. This latter aspect combined with its high concentration of dissolved organic carbon has make urine an ideal fuel to be treated by the technology [14] which led research focusing on the treatment of diverted urine. More specifically, on the development of autonomous sanitation system for decentralised areas [15–17]. During the progress and field testing of systems for this application, two main designs were developed, namely "two-chamber" ceramic based MFCs (**c**-MFC) [15,18] and "single-chamber" stratifying membrane-less MFCs (**s**-MFC) [19,20]. If both designs were developed to maximise the surface area of electroactive interfaces per volume of reactor, the key difference is the presence or absence of a membrane.

The ***c***-MFCs mounted with ceramic membranes were proved to be as efficient as MFC mounted with ion exchange membranes [21,22], which open the path of an economically viable implementation. The presence of a membrane enables a separation of the electrolyte into two types known as catholyte and anolyte. The produced catholyte (Fig. 1, "red" zone in the cylinder) has been proven to have bactericidal properties [23,24] and to concentrate certain elements such as potassium and sodium, a property that opens new potential applications as its can potentially enable the production of added-value products. In opposition, the ***s***-MFCs do not enable the separation of the treated waste into two different electrolytes. But as ***s***-MFC do not integrate membranes in their design, they have a higher surface area of electroactive interfaces per volume of reactor which results in simpler and cheaper bioreactors [19]. Although simpler, the ***s***-MFC designs are amongst the most power-dense systems that have reached field testing [16,17]. A recent study performed a side-to-side investigation of urine-fed ***c***-MFCs and ***s***-MFCs with an identical design as the one used here and which shared a maximum of common parameters in their design (i.e. HRT, electrodes total surface areas; electronic loads) [25]. Results have shown that, independently from the hydraulic retention time (HRT), the ***c***-MFCs had a relatively constant power output whilst ***s***-MFCs had a relatively constant energy conversion efficiency. Overall, results suggested that ***c***-MFCs were more appropriate for longer HRT and ***s***-MFCs for shorter HRT.

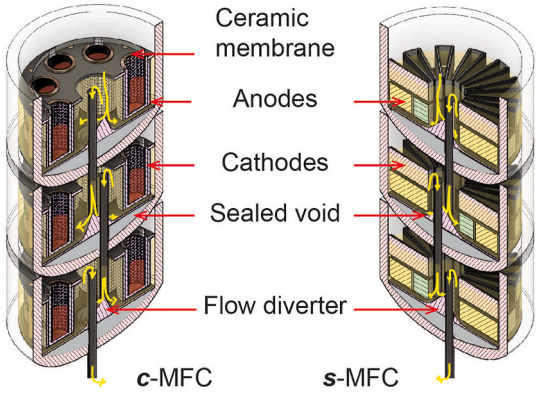

Fig. 1. Isometric and cross section view of the ceramic-based (**c**-MFC; left) and the membrane-less MFC (**s**-MFC; right) cascades, with both cascades comprising 3 MFC modules. The yellow arrows indicate the flow direction of the feedstock. (For interpretation of the references to color in this figure legend, the reader is referred to the Web version of this article.)

In the context of autonomous sanitation in decentralised areas, waterless urinal technologies present the advantage of limiting the pressure on a scarce resource, water. However, hygiene requires introducing some water in such systems for flushing to maintain cleanliness. Following up on the previous investigation [25] and keeping the focus towards practical implementation, the present study aims at examining the impact of urine dilution on the performance of the two types of designs, ***c***-MFC and ***s***-MFC. Here, the MFCs were arranged in cascades, the configuration utilised when the MFC technology is deployed in field applications [15–17]. Moreover, these two MFC designs had roughly similar parameters and operating conditions. The objective was to measure the power output and the treatment performance of these two cascade designs when fed increasingly diluted urine. This enables a deeper understanding of the impact water addition has in systems designed for treating undiluted urine, regarding COD and ammonium removal rates.

2. Experimental

2.1. Microbial fuel cells

The ***c***-MFC and ***s***-MFC modules employed here were of the same design as the ones used for the previous study [25]. Each ***c***-MFC module comprised of 8 individual earthenware ceramic cylinders (Laufen, Switzerland) that were enclosed in a cylindrical PVC vessel (Fig. 1). Each ***s***-MFC modules comprised 28 anode-cathode pairs enclosed in an identical cylindrical PVC vessel (Fig. 1). Most design parameters were similar with an anode surface area of 10,080 cm^2 (10 g m^{-2} carbon veil), a cathode surface area of 248 cm^2 (***c***-MFC) and 263 cm^2 (***s***-MFC), and a activated carbon loading on the anodes of 1.25 ± 0.1 mg cm^{-2} (***c***-MFC) and 1.19 ± 0.2 mg cm^{-2} (***s***-MFC). The main difference was that the ***c***-MFC modules had a displacement volume of 435 ± 3 ml whilst the ***s***-MFC modules had a displacement volume of 525 ± 4 ml. For more detail on the characteristic of each design, please refer to the previous study [25]. Three modules of each design were stacked one over the other to form a cascade taking the same footprint (Fig. 1), with a total displacement volume of 1.305 L for the ***c***-MFC cascade and 1.575 L for the ***s***-MFC cascade. A cascade is defined as a set of modules where the effluent of one module feeds into the next downstream module. A flow diverter was present at the bottom of each module to homogenise the feedstock distribution from the centre to the sides. The experiment consists of two cascades of three modules. The three modules within a cascade were electrically connected in parallel.

2.2. Operating conditions

Both cascades comprised modules that had been matured for more than a year and were fed urine that was collected daily from a tank pooling together the urine donated by anonymous individuals. The fed urine had gone through partial hydrolysis resulting in increased pH

ranging between 8.2 and 8.9. Following results from the previous study on the impact of the hydraulic retention time [25], each module had an aimed HRT of 12h resulting in both cascade having a HRT of approximatively 36h. Both cascades were connected to the same multichannel peristaltic pump giving the same flow rate of 0.66 mL min^{-1}. However, the modules (having a slightly different displacement volume) gave a different HRT for each cascade being 32.7h and 39.6h for the ***c***-MFC and *s*-MFC, respectively. Both cascades had its own feedline, but each feedline was connected to a common feeding tank that was continuously replenished with the collected urine, at room temperature (22 ± 1 °C). The investigated conditions were 100% urine, 75% urine, 50% urine and 25% urine. The dilution was made using tap water instead of distilled water to create conditions close to what could occur under real conditions of use. The dilutions were made by volume. For example, the 75% condition has a feedstock comprising 75% urine and 25% tap water (v/v).

2.3. Data capture

Throughout the duration of the experiment the cascades were connected to purpose-built circuitry maintaining potentiostatic conditions at 400 mV. This electronic board converted the measured current into voltage, which was recorded by an Agilent Data Acquisition System (Agilent LXI 34972A; Farnell, UK). More details on the circuitry is reported in a previous publication [26]. Measurements were recorded every 5 min. The current I in Amperes (A) was calculated using conversion formula, I =(Vm)/19.8, where V is the measured voltage in Volts (Vm) and 19,8 the conversion factor measured for the electronic board. The power output P in Watts (W) was calculated as $P = I \times V$, where V is the constant voltage (400 mV) in Volts (V) and I the measured current.

At the end of each incubation conditions, the COD and ammonium concentrations were measured, prior to shifting towards a new condition. The COD analyses were performed through the potassium dichromate oxidation method (COD HR test vials, Camlab, UK) with 0.2 mL of filtered (0.45 μm, Syringe Filter, Millipore) inlet and outlet samples. The ammonium concentration was determined by colorimetric analyses on diluted samples (1/20-1/100) using tablet reagents (Lovibond, UK) and an MD 500 colorimeter (Lovibond, UK).

The duplicates samples of the inlet were taken from the inlet tubing that was feeding each cascade. Output samples were taken from the outlet of each cascade. Each duplicate measured was averaged and the error bars present in the results figures stand for the data range. The error bars for the current and power results were calculated from the data points that covered the entirety of run ($\Delta t \approx 140$h; n ≈ 1,680).

To have a better understanding of the cascade performance, the electrical output was converted in KJ.d^{-1} and the organic carbon removed converted in the quantity removed per day ($g_{COD}.d^{-1}$). The electrical output of the last day of each incubation condition was used for these conversions. The normalised energy recovery (NER) [27,28] was also calculated to enable comparing the performance and behaviour of the two dissimilar systems tested here. The NER evaluates the proportion of electrical energy recovered from the feedstock, either in relation to the amount of organic matter present (NER_{COD}, based on COD measures) or in relation to the volume of wastewater treated (NER_V). The following equations were used to calculate both conversion factors:

$$NER_{COD}\ \left[KWh.Kg_{COD}^{-1}\right] = \frac{P\ [KW] \times t_{treatment}\ [h]}{V_{Treated\ during\ t}[m^3] \times \Delta COD\ [Kg_{COD}.m^{-3}]} \quad \text{eq. (1)}$$

$$NER_V\ \left[KWh.m^{-3}\right] = \frac{P\ [KW] \times t_{treatment}\ [h]}{V_{Treated\ during\ t}[m^3]} \quad \text{eq. (2)}$$

The power *P* corresponded to average power produced during the last 24h of each incubating condition, the time *t* corresponded to the HRT respective of each cascade, the volume *V* corresponded to the displacement volume of each cascade, and the amount of organic carbon removed *ΔCOD* corresponded to the difference of COD between the inlet and the outlet of each cascade and was measured at the end of each incubating condition.

3. Results and discussions

3.1. Electrical outputs

The ***c***-MFC and ***s***-MFC cascades were electrically connected in parallel whilst the urine was sequentially treated through the three successive modules of each cascade (Fig. 1). Overall, results indicate that both cascades displayed a similar behaviour towards urine dilution. The electrical outputs decreased with increasing dilution of the feedstock with the current outputs of the 100% > 75% > 50% > 25% (Fig. 2). Over the 140h of the experimental run, the variation of the current output was roughly 7-fold higher for the ***s***-MFC cascade compared to the ***c***-MFC. This result eches finding from the previous study on the behaviour of these two designs toward the variation of HRT [25].

The observed variability of the current output under constant incubating condition is hypothesised to result from the design of each type of cascade. Although the presence of a membrane adds resistance to the electrochemical reaction occurring in the dual compartment MFCs [29], which could explain the lower current output, the membrane brings stability by having separated reactive compartment (i.e. anodic and cathodic). Here, the porous ceramic membrane (≈16–22% of porosity; [30]) slows the diffusion of chemical elements from one side to the other, thus, delays the impact of the anolyte variations on the cathodic reactions. This is well illustrated by the current output of the ***c-MFC*** cascade which displays little current variation independently from the incubating conditions (Fig. 2a), implying that the difference of redox state between the compartments is maintained, along with the hypothesis that the substrate for the electroactive microbial populations is not limiting. The current output variation for all incubating conditions ranges from ±1.0 mA to ±2.2 mA. Moreover, the overall impact of the urine dilution seems to have less impact on the ***c-MFC*** with roughly *23.*4 mA difference between the 100% and the 25% condition (Fig. 2a).

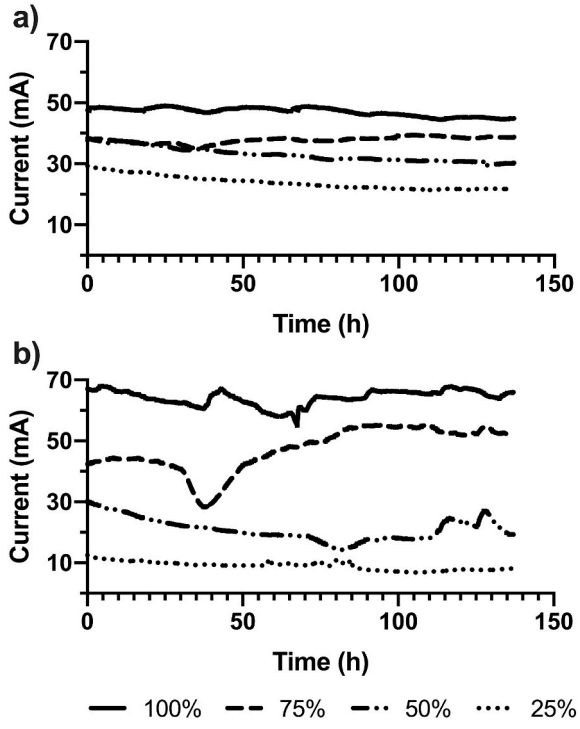

Fig. 2. Temporal absolute current and power outputs of the **c**-MFC (**a**) and **s**-MFC (**b**) cascades depending on the dilution rate of the urine feed stock, from 100% (no dilution) to 25% dilution (25% urine v/v).

Conversely to the ***c***-MFC cascade, the ***s***-MFC cascade displayed higher current output variation under each of the incubating condition, from ±1.3 mA to ±7.1 mA (Fig. 2b), similarly to previous results [25]. The specificity of the ***s***-MFC employed here is that the design exploits the self-stratification phenomenon that occurs in undisturbed water column. In such environment, chemical gradients develop under the activity of biological populations and results in the division of the water column in horizontal layers, each characterised by specific bio-chemical conditions (i.e. redox state of chemical elements, type of dominating metabolic activity) [31,32]. Exploiting this phenomenon in the MFC technology results in development of an autogenic transient chemical membrane between two major and distinct biochemical environments, an oxic top layer (cathodic environment) and an anoxic bottom layer (anodic environment). In ***s***-MFC the top layer comprises a plurality of partially submerged vertical cathodes whilst the bottom layer comprises a plurality of submerged vertical anodes. In ***s***-MFC the cathode and anode share the same electrolyte and are usually between 3 and 8 mm apart [20,26,33]. When considering that specific design feature, it is understandable that the performance of the ***s***-MFC is directly linked to the stability of its bioelectrochemical stratification of the urine column. Hence, any variation of the electrolyte composition would impact the current output of the ***s***-MFC. Results support this hypothesis as the urine dilution seems to have a high impact on the current output of the ***s***-MFC with roughly a 55.3 mA difference between the 100% and the 25% condition (Fig. 2b). These results imply that in ***s***-MFC, the gradients of diluted feedstocks are less efficient in maintaining an optimum redox difference between the anodic and cathodic layers, which results in lower electrical performance.

In the previous study [25], these designs were single module run under different HRT (3h, 6h, 12h, 24h, 65) and fed undiluted artificial urine media. Following the linear section of the curve between the 24h and the 65h HRT from these previous results, under the 32.7h HRT seen by the cascade in the present study, a single ***c***-MFC module would have continuously produced 6.45 mW, whilst a single ***s***-MFC module 7.80 mW under a 39.6h HRT. In the present study, a cascade of three modules under similar conditions produced 17.99 ± 0.10 mW and 26.45 ± 0.46 mW for the ***c***-MFC and the ***s***-MFC, respectively. This correspond to roughly three times the power produced by a single module in the previous study, 19.36 mW and 23.43 mW for the ***c***-MFC and the ***s***-MFC respectively. This similitude suggests that projections of power outputs can be employed to evaluate the power output of a cascade, at least when the HRT between a single module and a cascade are matched.

Depending on the incubating conditions, the current outputs ranged between 23.7 ± 2.1 mA and 47.1 ± 1.4 mA for the **c**-MFC cascade and 8.9 ± 1.2 mA and 64.2 ± 2.6 mA for the **s**-MFC cascade. The level and the variation range of the current outputs are dictated by the bioreactor designs and prevent a direct comparison of the behaviours. Since the currents tend to decrease with increasing dilution, the current output of each cascade was converted in the percentage of its respective output when fed undiluted urine (Fig. 3). This to facilitate the identification of the trends specific to each design without being masked by the specific value of the current outputs.

The average current output of the ***c***-MFC cascade decreased by 19 ± 2% under the 75% incubating condition compared to the undiluted condition (Fig. 3). At 50% urine, the current output decreased by 29 ± 5%, and at 25% urine the decrease was of 49 ± 5%. Although the urine composition changes between each incubating conditions due to the unknown donation patterns, the relation between the current output and the feedstock dilution are negatively correlated ($R^2 = 0.9866$). In comparison the average current output of the ***s***-MFC cascade decreased much more than the ***c***-MFC (Fig. 3). As for the ***c***-MFC cascade, the ***s***-MFC cascade current output was negatively correlated to the feedstock dilution ($R^2 = 0.9822$). The decrease of the ***s***-MFC cascade was roughly twice higher (trendline $a \approx 120$) than the one of the ***c***-MFC cascade (trendline $a \approx 63$). Overall, the results have shown that the current output of the ***s***-MFC cascade was higher than the ***c***-MFC cascade with

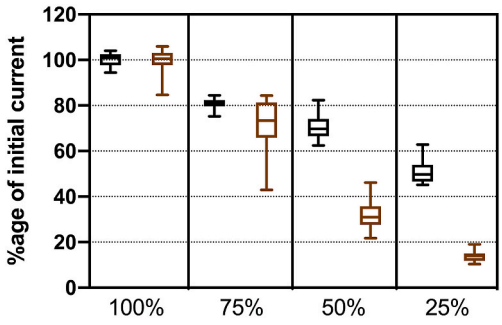

Fig. 3. Relative current output of the **c**-MFC (**black**) and **s**-MFC (**brown**) cascades depending on the dilution rate of the urine feed stock. The relative current output is calculated in percentage of the current produced when there is no dilution of the urine (100%). (For interpretation of the references to color in this figure legend, the reader is referred to the Web version of this article.)

undiluted urine, but due to the presence of a membrane, the ***c***-MFC cascade had a more stable output (Figs. 2 and 3). Moreover, the level of current output of the ***c***-MFC cascade was less affected by the dilution of the feedstock compared to the ***s***-MFC (Figs. 2 and 3). This is likely because of the presence of the separator between the anodic and cathodic compartments that limited the ingress of oxygen in the anaerobic anodic compartment. Overall, such decrease in electrical output was to be expected from MFC cascades acclimated to high strength feedstock. The decrease of the electrical output can be attributed to the decrease of both the electroconductivity (e.g. 28.3 mS cm^{-2} at 100% and 9.65 mS cm^{-2} at 25%) and the lower COD concentration.

3.2. *Treatment performance*

Both the ***c***-MFC and ***s***-MFC cascades were fed urine from the undiluted condition to the 25% dilution conditions. After running the cascades under the four investigated conditions (i.e. 100%, 75%, 50%, 25%), both cascades were run under a 100% condition for 2 days and the effluent analyse, as a control, to compare results to the initial undiluted run (i.e. 100%). The analyses focused on the ammonium and chemical oxygen demand (COD). The effluents were sampled at the end of each run of the investigated conditions.

Between the two 100% runs, the partially hydrolysed urine feedstock contained an average of 5,085 ± 254 $mg_{COD}.L^{-1}$. Compared to this average, the diluted feedstocks contained 66%, 53% and 25% COD for the 75%, 50%, and 25% conditions, respectively. Conversely to the organic loading, the ammonium loading showed higher variation between the first and second run under the 100% condition with an average concentration of 5,727 ± 664 $mg_{NH4}.L^{-1}$. For the ***c***-MFC cascade, the ammonium and organic removal rates were of 12% and 17% for the first run at 100% (Fig. 4a), 10% and 16% for the second run at 100%, respectively (data not shown). The ***s***-MFC cascade displayed an ammonium and an organic removal rate of 23% and 63% for the first run at 100% (Figs. 4a), 17% and 68% for the second run at 100%, respectively (data not shown). These results indicate that the ammonium and organic loading removal rates were in the same range under replicated incubating conditions (i.e. undiluted urine), thus, supporting the results of the other incubating conditions that were only run once.

Although the ammonium and COD concentration of the inlets are in the same range, the measurements indicate that both cascade designs had organic carbon removal rates higher than their respective ammonium removal rates. An observation valid for all incubating conditions (Fig. 4). For the ***c***-MFC cascade, the ammonium removal rate decreases as the feedstock concentration decreases (Fig. 4). Although the ***s***-MFC cascade displayed higher ammonium removal rates, the same trend was observed (Fig. 4). Conversely to the ammonium removal, the ***c***-MFC cascade displayed higher COD removal rate as the feedstock concentration decreased (Fig. 4). Similarly, the COD removal rates of the ***s***-MFC

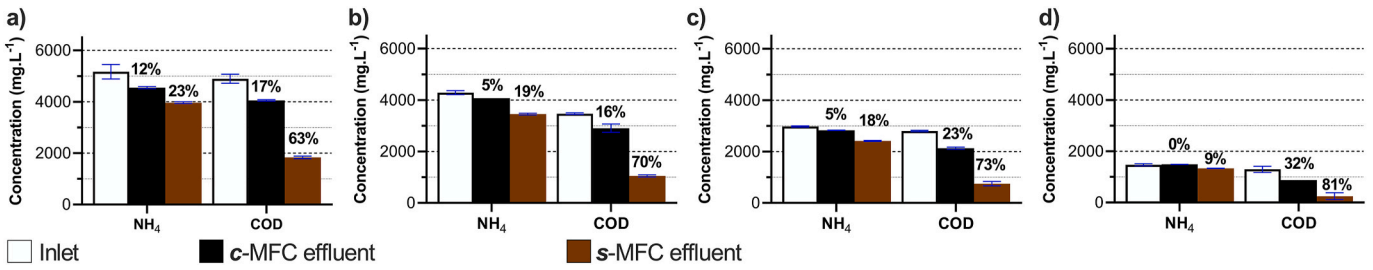

Fig. 4. Ammonium and COD concentrations of the feed stock (**white**) and the effluent of the **c**-MFC (**black**) and **s**-MFC (**brown**) cascades depending on the dilution rate of the urine feed stock: 100% urine (**a**), 75% urine (**b**), 50% urine (**c**), and 25% urine (**d**). (For interpretation of the references to color in this figure legend, the reader is referred to the Web version of this article.)

cascade were higher for feedstock with lower concentrations, (Fig. 4). These responses are indicative that both the ammonium and COD concentrations of the feedstock are correlated to the removal rates displayed by the cascades. In the previous study [25] these designs were single module run under different HRT (3h, 6h, 12h, 24h, 65) and fed artificial urine media. Projections from these previous results indicated that under a 32.7h HRT and a 39.6h HRT, a ***c***-MFC and a ***s***-MFC modules would have removed 7.61% and 34.36% COD, respectively. Compared to the 100% condition, results demonstrate that under the similar HRT the cascade configuration enables a higher treatment efficiency with COD removal rates of 17% and 63% for the ***c***-MFC and ***s***-MFC cascades, respectively.

The removal rates for each incubating condition were plotted against the feedstock concentration to better visualise a potential correlation between concentrations and treatment performance (Fig. 5). Overall, the ***s***-MFC has on average a three-fold higher ammonium and COD removal rates compared to the ***c***-MFC cascade. Interestingly, the trendline's slope of both cascades are very similar with values of 0.0035 (***s***-MFC) and 0.0025 (***c***-MFC) for the ammonium and of −0.0052 (***s***-MFC) and −0.0044 (***c***-MFC) for the COD. The correlation test performed on the ammonium data indicates a p(two-tailed) of 0.0021 and 0.0005 and a R^2 of 0.8159 and 0.8814 for the ***c***-MFC and ***s***-MFC cascades, respectively (Fig. 5a). The correlation test performed on the COD data indicates a p(two-tailed) of 0.0025 and < 0.0001 and a R^2 of 0.8060 and 0.9976 for the ***c***-MFC and ***s***-MFC cascades, respectively (Fig. 5b). These results clearly indicate that there is a correlation between the feedstock concentration and the treatment performance of the cascades, a positive correlation in the case of the ammonium and negative correlation in the case of the COD.

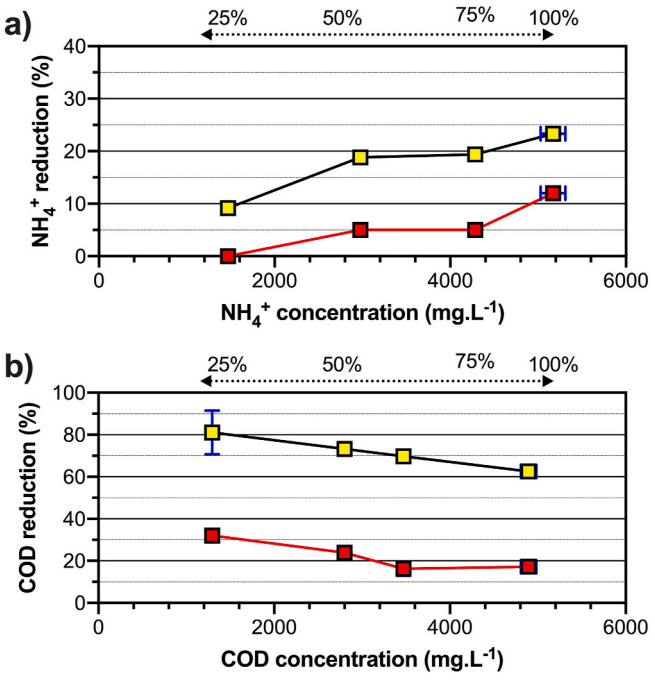

Fig. 5. Correlation between the feedstock concentration and the observed removal rates for the ammonium (**a**) and the COD (**b**). **Red** stands for the **c**-MFC and **yellow** for the **s**-MFC. (For interpretation of the references to color in this figure legend, the reader is referred to the Web version of this article.)

Previous research on ***c***-MFC have shown that the catholyte production and ammonium removal in a ceramic based microbial fuel cell was linked to the transport of the positive charge into the cathode and an electro-osmotic drag phenomenon [34]. This results in the ammonium ion migrating towards the cathode dragging molecules of water, where it exits the reactor as ammonia due to the alkaline pH of catholyte (Ammonia–Ammonium pKa = 9.25) generated by oxygen reduction reaction (ORR). Since the continuous cathodic ORR reaction increases the catholyte pH to a level that was higher than the ammonia pKa value, the concentration of free ammonia in the catholyte increased enabling ammonia volatilising from the liquid phase to the gaseous phase [35]. The catholyte pH increases with higher ceramic thickness and higher current, which leads to higher ammonium removal [34,36]. Therefore, the lower ammonium removal rate observed in ***c***-MFC under diluted conditions could be attributed to lower conductivity of the electrolyte and lower COD concentration that resulted in lower power (Fig. 5a). Regarding ***s***-MFC, there are very little data available on the biological and electrochemical reactions occurring within such reactors, especially regarding the nitrogen cycle. The only reported understanding are that the cathodic biofilm are essential for ***s***-MFC to operate [20], and that there is an anaerobic ammonium abstraction occurring in the cathodic bottom layer, just above the redoxcline separating cathodes and anodes [19]. Hence, it is difficult to explain why the ammonium removal rates decrease under diluted conditions (Fig. 5a). If the removal was to be biological, a potential cause for lower removal rate could relate to the microorganisms having a low affinity for the substratum. Another possibility would be that the reaction is purely electrochemical, thus, depending on the concentration and the electrochemical activity of the cells, where the separation process uses the advantage of current production by the MFC, which drives ammonium transport from the anodic to the cathodic environment. However, it should be considered that the pH of the electrolyte in the cathodic layer in ***s***-MFC is relatively low (pH ≈ 8.3–9.0) compared to ***c***-MFC (9.5–10.8). Hence, it can be postulated that ammonium stripping due to the pH is less marked for ***s***-MFC because of the lower pH.

Conversely to the positive correlation between the ammonium concentration and the removal rates, the COD removal rate is negatively correlated to the COD concentration (Fig. 5b). These results show that the treatment was more efficient at a lower substrate concentration, a behaviour observed in previous studies [37,38]. The reported rates are the percentage decrease in relation to the input concentration. This increase indicates that a higher proportion of a more diluted feedstock was removed. In addition to the lower COD concentration, the other elements are also in lower concentration and ammonium is known to

inhibit the activity of some electroactive microorganisms [39]. Both cascades were matured under high-strength feedstock, thus, they comprised ammonium tolerant population. However, results suggest that the enriched microbial populations also contained heterotrophic communities that were inhibited by the high ammonium concentration. The increasing COD removal rates with increasingly diluted feedstock support the hypothesis that as the ammonium concentration decreased, microbial communities with higher affinity for their substrate were greater in number and/or more active.

3.3. Conversion efficiency and energy recovery

The ***s***-MFC cascade displayed higher performance than ***c***-MFC cascade in terms of treatment for all incubating conditions (Figs. 4–6), and in terms of energy output for the 100% and 75% conditions (Figs. 2 and 6). However, the energy output of the ***s***-MFC cascade under the 50% and 25% were lower than ***c***-MFC cascade, although their treatment was 2.75-fold higher. These raw data on the performance were normalised to better appreciate the efficiency of both designs. The first data conversion focused on the relation between the quantity of energy generated in 24h and the quantity of COD removed within the same time interval, considering their specific HRT and displacement volume (Fig. 6a). This normalisation was performed using the data from the last 24h of each incubating conditions, when the COD and Ammonium concentrations were measured. The ***c***-MFC displayed a narrow variation of its daily energy production with a 0.80 ± 0.01 kJ d^{-1} difference. Conversely, the ***s***-MFC cascade had a wider variation gap with a difference of 2.02 ± 0.08 kJ d^{-1} in its daily energy production. The daily energy production reflect the results shown in Fig. 2 with a delta of 0.80 kJ d^{-1} for ***c***-MFC and a delta of 2.02 KJ.$d^{-1}$for the ***s***-MFC cascade (Fig. 6a). Similarly, the ***s***-MFC cascade displayed a wide variation in the quantity of COD daily removed with a delta of 2.95 ± 0.15 g_{COD}.d^{-1}. Comparatively the ***c***-MFC cascade displayed a delta of 0.41 ± 0.15 g_{COD}.d^{-1}. (Fig. 6a). The conversion ratio between the daily energy and quantity of COD removed are of 1.90 KJ.g_{COD}^{-1} and 0.55 KJ.g_{COD}^{-1} for the ***c***-MFC and ***s***-MFC cascades under the 100% condition, respectively. Although the ratios are lower compared to the previous investigation [25], they similarly indicate that the ***c***-MFC cascade has a higher conversion efficiency than the ***s***-MFC cascade. The lower conversion efficiency of the ***s***-MFC cascade, together with its higher COD removal rate (Fig. 6a) indicates that part of the organic matter is not mineralised by the electroactive communities. This observation supports the hypothesis that part of this organic matter mineralisation could result from the design having a higher surface exposed to air, and in particular the fact that the waste stream is in contact with the cathodic compartment half of the time. These results indicate that if the ***s***-MFC design has 3-fold higher performance (i.e. quantity of energy produced and/or of COD removed) it is 3-fold less efficient than the ***c***-MFC design in converting the available organic matter into electrical current.

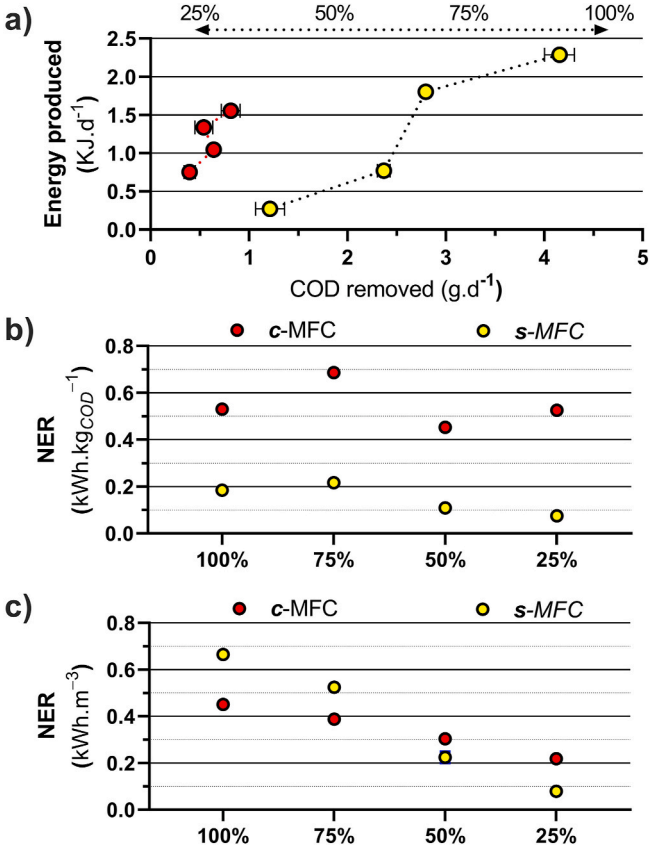

Fig. 6. (**a**) Correlation between the energy produced and the quantity of COD removed in 24h. **Red** stands for the **c**-MFC and **yellow** for the **s**-MFC. (**b**, **c**) Normalised energy recovery rates depending on the incubating condition: (**b**) NER_{COD}, and (**c**) NER_V. (For interpretation of the references to color in this figure legend, the reader is referred to the Web version of this article.)

To continue evaluating the efficiency of the energy conversion, the Normalised Energy Recovery factors (NER) were calculated according to Refs. [27,28] (Fig. 6b and c). Again, these normalisations were performed using the last 24h of each incubating conditions, when the COD and ammonium concentrations were measured. The average NER_{COD} for the ***c***-MFC cascade was of 0.570 ± 0.004 KWh.Kg_{COD}^{-1} whilst the ***s***-MFC cascade displayed an average NER_{COD} of 0.147 ± 0.065 KWh.Kg_{COD}^{-1} (Fig. 6b). If NER_{COD} of the ***c***-MFC cascade do not appear to be correlated to the incubating condition (Fig. 6b), the NER_{COD} of the ***s***-MFC cascade appears to be correlated to the feedstock dilution: the higher the urine dilution, the lower the conversion efficiency. Compared to the previous study, the NER_{COD} of the ***c***-MFC under the 100% condition is here 3-fold lower (1.23 KWh.Kg_{COD}^{-1}, [25]) and the NER_{COD} of the ***s***-MFC cascade is 1.3-fold lower (0.309 KWh.Kg_{COD}^{-1}, [25]). This difference could be due to the nature of the feedstock between the two experiments. The previous study was carried out with artificial urine with peptone and yeast extract as the carbon source (artificial urine media), whereas here the carbon source was much more complex (undiluted human urine). Also, the previous results reported that the ***s***-MFC design had a stable NER_{COD} over the range of tested HRT conditions [25]. Here, NER_{COD} of the ***s***-MFC could be grouped into two categories of similar values, the 100% and 75% conditions with an average of 0.201 ± 0.023 KWh.Kg_{COD}^{-1}, and the 50% and 25% conditions with an average of 0.092 ± 0.024 KWh.Kg_{COD}^{-1} (Fig. 6b). Due to the nature of this design exploiting the natural stratification of the urine column, these results indicate that the ***s***-MFC cascade shifted from one equilibrium to another. The second equilibrium being marked by half the NER_{COD}, whilst having a higher COD removal rate, could be indicative of a decreasing activity of electroactive microorganisms but an increasing activity of the none electroactive heterotrophic species (Fig. 6a and b).

Interestingly, the NER_V of both cascades were very similar to the ones of the previous study [25]. Here, the ***c***-MFC cascade had a NER_V of 0.451 ± 0.003 KWh.m^{-3} (i.e. previously ≈0.454 KWh.m^{-3}) and the ***s***-MFC cascade had a NER_V of 0.665 ± 0.012 KWh.m^{-3} (i.e. previously ≈0.551 KWh.m^{-3}) (Fig. 6c). Conversely, to the NER_{COD} the NER_V display a positive correlation with the feedstock concentration for both cascade designs. Under the 100% and 75% condition the NER_V of the ***s***-MFC cascade was higher than the ***c***-MFC cascade, whilst under the 50% and 25% condition the ***c***-MFC cascade was higher than the ***s***-MFC cascade. The slopes of the NER_V correlation to the incubating condition was similar to the current output behaviour (Fig. 3) with the ***s***-MFC having a higher slope than the ***c***-MFC, indicating that the ***c***-MFC was more resilient towards high feedstock dilutions. Compared to other studies [27,40], both the ***c***-MFC and ***s***-MFC cascades showed, under the 100% condition, lower NER_{COD} (max reported: 1.35 KWh.Kg_{COD}^{-1}, [40]; 2.092 KWh.Kg_{COD}^{-1}, [25]) but much higher NER_V (max reported: 0.380

KWh.m^{-3}, [40]).

4. Conclusion

This study investigates the response of two different MFC designs to the dilution of feedstock by tap water from 100%, 75%, 50%–25% urine. Both the ***c***-MFC and ***s***-MFC displayed a decreasing current output with increasing dilution. The ***c***-MFC had a lower current output but was less impacted by increasing dilutions. The ***s***-MFC cascade had a higher output but showed up to 86 ± 2% decrease in output under the 25% condition. These results indicate that the presence of a membrane increased the resilience toward dilution. Both the ***c***-MFC and ***s***-MFC displayed an ammonium removal rate positively correlated to the concentration. The ***s***-MFC displayed ammonium removal rates roughly 3-fold higher than the ***c***-MFC for all the tested conditions. These results suggest that the ammonium removal is mainly linked to an electrochemical reaction in ***c***-MFC, whereas it could only account for part of the ammonium removal observed in ***s***-MFC. Both the ***c***-MFC and ***s***-MFC displayed a COD removal rate negatively correlated to the concentration. The ***s***-MFC displayed COD removal rates roughly 4-fold higher than the ***c***-MFC. These results suggest that the ammonium concentration decrease favour the activity of heterotrophic microorganisms with a high affinity for their substrate.

The ***s***-MFC displayed roughly 3-fold higher daily COD removal rates than the ***c***-MFC under the 50% and 25% conditions, but at the same time displayed roughly 2-fold lower daily energy production compared to the ***c***-MFC. The ***c***-MFC displayed 3- to 7-fold higher energy conversion efficiency (NER_{COD}, $KWh.Kg_{COD}^{-1}$) under all tested conditions. Under the 100% and 75% conditions, the ***s***-MFC exhibited a 47% and 35% higher volumetric energy recovery (NER_V, KWh.m^{-3}), respectively. Under the 100% and 75% conditions, the ***c***-MFC exhibited a 35% and 178% higher volumetric energy recovery. These results demonstrate that overall, the ***c***-MFC have a higher energy conversion efficiency than the ***s***-MFC. Moreover, these results suggest that the presence of a membrane optimises the enrichment of electroactive heterotrophs, whereas self-stratifying setup have a more diverse population of heterotrophs with some not being electroactive. However, results suggest that the absence of membrane, and subsequent potential diversity of heterotrophs, lead to higher performance in normal conditions whilst being more sensitive to perturbation.

The Technology Readiness Level (TRL) and potential for commercialisation of MFC are of particular interest since the major challenges in scaling-up the technology are related to the factors governing manufacturing processes. Most elements, materials and processes are expensive therefore the efforts of using alternative solutions such as use of ceramic membranes or a membrane-less solutions is being presented in this work as one way towards field applicable MFC systems. Because of an alternative approach, this work has the potential to support the technology higher TRL (7–9) and real-world implementation feasibility. Indeed, both design concepts (i.e. ceramic cylindrical membrane with internal cathode; and membrane less self-stratifying setups) have been successfully tested in pilot-scale trials illustrating a potential pragmatic route for implementation [15–17,41]. However, to fully validate these development routes, a life cycle assessment study should be performed along with an economical analysis of the production, the deployment, and the operation of large systems.

Overall and in regard of hygiene in the maintenance of waterless urinal, results indicate that both designs can handle a dilution up to 75% urine without a significant performance decrease.

CRediT authorship contribution statement

Xavier Alexis Walter: Supervision, Conceptualization, Methodology, Investigation, Data curation, Formal analysis, Analysis and Interpretation, Writing – original draft, Writing – review & editing. **Jiseon You:** Investigation, Formal analysis, Analysis and Interpretation, Writing – review & editing. **Iwona Gajda:** Methodology, Investigation, Analysis and Interpretation, Writing – review & editing. **John Greenman:** Supervision, Writing – review & editing. **Ioannis Ieropoulos:** Principal Investigator, Funding acquisition, Supervision, Writing – review & editing.

Declaration of competing interest

The authors declare that they have no known competing financial interests or personal relationships that could have appeared to influence the work reported in this paper.

Data availability

Data will be made available on request.

Acknowledgment

The authors would like to acknowledge the Bill & Melinda Gates Foundation for funding the scientific work (Seattle, WA; grant no. OPP1149065).

References

[1] M.C. Potter, Proc. R. Soc. B 84 (1911) 260–276.
[2] D. Czerwińska-Główka, K. Krukiewicz, Bioelectrochemistry (2020) 131.
[3] C. Santoro, C. Arbizzani, B. Erable, I. Ieropoulos, J. Power Sources 356 (2017) 225–244.
[4] L. Su, W. Jia, C. Hou, Y. Lei, Biosens. Bioelectron. 26 (2011) 1788–1799.
[5] M.H. Do, H.H. Ngo, W. Guo, S.W. Chang, D.D. Nguyen, Y. Liu, et al., Sci. Total Environ. 712 (2020), 135612.
[6] X. Cao, X. Huang, P. Liang, K. Xiao, Y. Zhou, X. Zhang, et al., Environ. Sci. Technol. 43 (2009) 7148–7152.
[7] M. Ramírez-Moreno, A. Esteve-Núñez, J.M. Ortiz, Electrochim. Acta 388 (2021), 138570.
[8] P. Kuntke, K.M. Smiech, H. Bruning, G. Zeeman, M. Saakes, T.H.J.A. Sleutels, et al., Water Res. 46 (2012) 2627–2636.
[9] B.E. Logan, D. Call, S. Cheng, H.V.M. Hamelers, T.H.J.A. Sleutels, A.W. Jeremiasse, et al., Environ. Sci. Technol. 42 (2008) 8630–8640.
[10] J. Hnát, M. Paidar, K. Bouzek, in: A. Iulianelli, A. Basile (Eds.), Current Trends and Future Developments on (Bio-) Membranes, Elsevier, 2020, pp. 91–117.
[11] T.M.P. Martin, F. Esculier, F. Levavasseur, S. Houot, Crit. Rev. Environ. Sci. Technol. 52 (2022) 890–936.
[12] T. A. Larsen , W. Gujer, 1996;34:87-94.
[13] M. Maurer, P. Schwegler, T.A. Larsen, Water Sci. Technol. 48 (2003) 37–46.
[14] I. Ieropoulos, J. Greenman, C. Melhuish, Phys. Chem. Chem. Phys. 14 (2012) 94–98.
[15] I.A. Ieropoulos, A. Stinchcombe, I. Gajda, S. Forbes, I. Merino-Jimenez, G. Pasternak, et al., Environ. Sci.Water.Res. Technol. 2 (2016) 336–343.
[16] X.A. Walter, I. Merino-Jiménez, J. Greenman, I. Ieropoulos, J. Power Sources 392 (2018) 150–158.
[17] X.A. Walter, J. You, J. Winfield, U. Bajarunas, J. Greenman, I.A. Ieropoulos, Appl. Energy 277 (2020), 115514.
[18] I. Gajda, A. Stinchcombe, J. Greenman, C. Melhuish, I. Ieropoulos, Int. J. Hydrogen Energy 40 (2015) 14627–14631.
[19] X.A. Walter, I. Gajda, S. Forbes, J. Winfield, J. Greenman, I. Ieropoulos, Biotechnol. Biofuels 9 (2016) 93.
[20] X.A. Walter, C. Santoro, J. Greenman, I.A. Ieropoulos, Bioelectrochem. 133 (2020), 107491.
[21] J. Winfield, J. Greenman, D. Huson, I.A. Ieropoulos, Bioproc. Biosyst. Eng 36 (2013) 1913–1921.
[22] J. Winfield, I. Gajda, J. Greenman, I.A. Ieropoulos, Bioresour Technol 215 (2016) 296–303.
[23] I. Gajda, J. Greenman, C. Melhuish, I.A. Ieropoulos, Sci. Rep. 6 (2016).
[24] I. Merino-Jimenez, O. Obata, G. Pasternak, I. Gajda, J. Greenman, I. Ieropoulos, Process Biochem. 101 (2021) 294–303.
[25] X.A. Walter, E. Madrid, I. Gajda, J. Greenman, I. Ieropoulos, J. Power Sources 520 (2022), 230875.
[26] X.A. Walter, C. Santoro, J. Greenman, I.A. Ieropoulos, Bioelectrochem. 127 (2019) 68–75.
[27] S. Zou, Z. He, Water Res. 131 (2018) 62–73.
[28] Z. Ge, J. Li, L. Xiao, Y. Tong, Z. He, Environ. Sci. Technol. Lett. 1 (2014) 137–141.
[29] J. Ramirez-Nava, M. Martínez-Castrejón, R.L. García-Mesino, J.A. López-Díaz, O. Talavera-Mendoza, A. Sarmiento-Villagrana, et al., Membranes 11 (2021) 738.
[30] M.J. Salar-García, I. Ieropoulos, J. Power Sources 451 (2020), 227741.
[31] X.A. Walter, Neuchâtel, Université de Neuchâtel, 2011 [PhD].
[32] X.A. Walter, A. Picazo-mozo, M.R. Miracle, E. Vicente, A. Camacho, A. Michel, et al., Front. Microbiol. 5 (2014).

[33] X.A. Walter, C. Santoro, J. Greenman, I. Ieropoulos, Int. J. Hydrogen Energy (2019) 4524–4532.
[34] I. Gajda, J. Greenman, C. Santoro, A. Serov, P. Atanassov, C. Melhuish, et al., J. Chem. Technol. Biotechnol. 94 (2019) 2098–2106.
[35] R. Cord-Ruwisch, Y. Law, K.Y. Cheng, Bioresour. Technol. 102 (2011) 9691–9696.
[36] I. Merino Jimenez, J. Greenman, I. Ieropoulos, Int. J. Hydrogen Energy 42 (2017) 1791–1799.
[37] S. Wu, P. Liang, C. Zhang, H. Li, K. Zuo, X. Huang, Electrochim. Acta 161 (2015) 245–251.
[38] J. You, J. Greenman, I. Ieropoulos, Energies 11 (2018) 12.
[39] A.B. Ergettie, M. Dagbasi, Biofuels 12 (2021) 655–661.
[40] N. Yang, Q. Zhou, G. Zhan, Y. Liu, H. Luo, D. Li, Sci. Total Environ. 788 (2021), 147652.
[41] J. You, C. Staddon, A. Cook, J. Walker, J. Boulton, W. Powell, et al., Int. J. Environ. Res. Publ. Health 17 (2020) 2175.